Progress In Electromagnetics Research M, Vol. 18, 119–130, 2011

THREE DIMENSIONAL ELECTROMAGNETIC CONCENTRATORS WITH HOMOGENEOUS MATERIAL PARAMETERS

T. Li, M. Huang*, J. Yang, S. Mu, and F. Mao

School of Information Science and Engineering, Yunnan University, Kunming 650091, China

Abstract—By means of a three-step linear optical transformation method, material parameters of a three-dimensional diamond-shaped electromagnetic concentrator composed of tetrahedral homogeneous blocks has been derived in this paper. The performance of the concentrator has been confirmed by full-wave simulation. The designed concentrator can operate in a wide bandwidth due to the line transformation. It represents an important progress towards the practical realization of the metamaterial-assisted concentrator.

1. INTRODUCTION

The idea of transformation optics generalized by Pendry et al. [1] has attracted keen interest in designing conceptual devices that can control electromagnetic waves with unprecedented degrees of freedom. The most interesting application of this idea might be the invisible cloaks [2–13], which can hide arbitrary objects from exterior electromagnetic illumination and suppress all the scattered waves. Besides, some other devices with novel functions have also been reported, such as imaging with unlimited resolution [14], field-rotating device [15], field concentrator [16], illusion device [17], superscatterer [18], beam splitter [19], and so on. Reviews of this large body of work have been provided by Jiang et al. [20] and Kwon and Werner [21]. Among various novel applications, the phenomenon of near-field concentration of light plays an important role in the harnessing of light in solar cells or similar devices, where high field intensities are required. Since the circular cylindrical electromagnetic

Received 7 April 2011, Accepted 9 May 2011, Scheduled 17 May 2011

* Corresponding author: Ming Huang (huangming@ynu.edu.cn).

concentrator was firstly proposed by Rahm et al. [16], much attention has been drawn to the design of concentrator based on transformation optics. Jiang et al. [22] presented the analytical design of arbitrary shaped concentrators, of which the geometry boundary is represented by a non-uniform rational B-spline. Yang et al. [23] derived the generalized material parameter equations for an arbitrary shaped electromagnetic concentrator, of which the contour can be described by a continuous function $R(\theta)$ with period 2π. Later, Yang et al. [24] developed an inverse method based on numerical solution of Laplace's equation to design irregular shaped concentrators. However, the practical fabrication of these concentrator devices has so far not been achievable, since the material parameters are usually highly anisotropic, inhomogeneous and even singular.

Recently, Li et al. [25] proposed a two dimensional homogeneous-materials-constructed electromagnetic field concentrator whose energy concentrating ratio varies with the incident angle of the electromagnetic wave. Although the two dimensional model can help us to understand the electromagnetic properties of the homogeneous concentrator, it is just the first step towards the realization of electromagnetic concentrator. Therefore, it is urgent to develop the three-dimensional (3D) concentrator with non-singular and homogeneous material parameters. Inspired by the work of Li et al. [25] and Wang et al. [26] who developed a three-step coordinate transformation method for designing invisible cloak, a 3D diamond-shaped concentrator composed of tetrahedral homogeneous blocks is presented in this paper. Permittivity and permeability of the concentrator is derived, and validated by numerical simulation. Compared with a traditional electromagnetic concentrator, material parameters of the concentrator are homogeneous and non-singular, which dramatically reduce the difficulty in practical implementation. Furthermore, we find that the 3D concentrator can operate in a wide spectral range, which is a key issue for the application of solar energy.

2. METHOD AND SIMULATION MODEL

According to the coordinate transformation method, under a space transformation from the original coordinate (x_1, x_2, x_3) to a new coordinate $(x_1'(x_1, x_2, x_3), x_2'(x_1, x_2, x_3), x_3'(x_1, x_2, x_3))$, the permittivity ε' and the permeability μ' in the transformed space are given by [27]

$$\varepsilon' = \mathbf{A}\varepsilon\mathbf{A}^T/\det\mathbf{A}, \quad \mu' = \mathbf{A}\mu\mathbf{A}^T/\det\mathbf{A} \tag{1}$$

where ε and μ are the permittivity and permeability of the original space. $\mathbf{A}$ is the Jacobian transformation matrix with components

$A_{ij} = \partial x_i'/\partial x_j$. It is the derivative of the transformed coordinates with respect to the original coordinates. $\det \mathbf{A}$ is the determinant of the matrix. The determination of matrix $\mathbf{A}$ is the key issue for designing the transformation medium.

The 3D diamond-shaped electromagnetic concentrator is divided into eight parts by the x, y, z coordinate axes. The schematic diagram of the coordinate transformation for the design of the first part of the 3D concentrator in the first quadrant is shown in Fig. 1. The other parts are axially symmetrical to the first part, and it is not shown here for brevity. Figs. 1(a)–(d) show the original Cartesian space (x, y, z), the transitional Cartesian space (x', y', z'), (x'', y'', z''), and the transformed Cartesian space (x''', y''', z'''), respectively. The 3D concentrator can be obtained through a three-step linear transformation. The first step (*step* 1) is to compress OD to OD' in the x-axis direction, while keeping the y-axis and z-axis undistorted. The second step (*step* 2) is similar to the *step* 1 but in the y direction, that is, to compress OE to OE'. The last step (*step* 3) is only to compress OF to OF' in the z direction. Let $OA = a$, $OB = b$, $OC = c$, $OD = d$, $OD' = d'$, $OE = e$, $OE' = e'$, $OF = f$, and $OF' = f'$. Transformation steps are described as follows.

In *step* 1, the original space (x, y, z) is transformed into the transitional space (x', y', z'). The region 1 (ABCD) in Fig. 1(a) is stretched into region 1 (ABCD′) in Fig. 1(b). Similarly, regions 2, 3 and 4 in Fig. 1(a) is compressed into the corresponding regions in Fig. 1(b). For each region, the coordinate transformation equations can be described as follows.

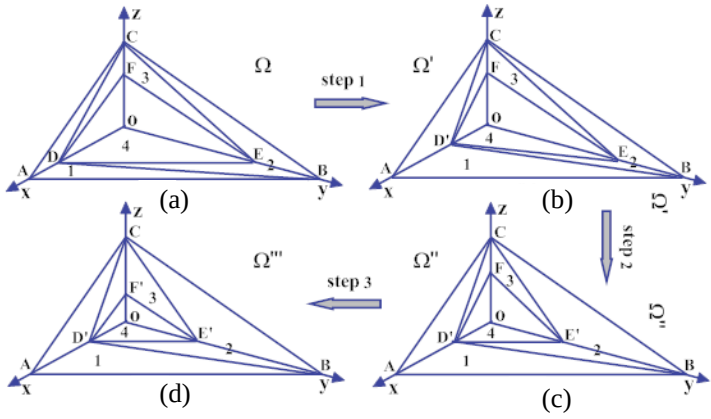

Figure 1. Schematic diagram of the coordinate transformation for the design of 3D concentrator.

Region 1:

$$x' = \frac{a-d'}{a-d}x - \frac{a(d-d')}{b(d-a)}y - \frac{a(d-d')}{c(d-a)}z + \frac{a(d-d')}{d-a},\ y' = y,\ z' = z \tag{2}$$

Region 2:

$$x' = \frac{d'}{d}x,\ y' = y,\ z' = z \tag{3}$$

Region 3:

$$x' = \frac{d'}{d}x,\ y' = y,\ z' = z \tag{4}$$

Region 4:

$$x' = \frac{d'}{d}x,\ y' = y,\ z' = z \tag{5}$$

In *step 2*, the transitional space (x', y', z') is transformed into (x'', y'', z''), and OE is compressed to OE' in the y direction. From Fig. 1(c), it can be seen that region 1 keeps unchanged; region 2 is stretched; regions 3 and 4 are relatively compressed. The corresponding mapping for each region can be expressed by the following equations.

Region 1:

$$x'' = x',\ y'' = y',\ z'' = z' \tag{6}$$

Region 2:

$$x'' = x',\ y'' = -\frac{b(e-e')}{d'(e-b)}x' + \frac{b-e'}{b-e}y' - \frac{b(e-e')}{c(e-b)}z' + \frac{b(e-e')}{e-b},\ z'' = z' \tag{7}$$

Region 3:

$$x'' = x',\ y'' = \frac{e'}{e}y',\ z'' = z' \tag{8}$$

Region 4:

$$x'' = x',\ y'' = \frac{e'}{e}y',\ z'' = z' \tag{9}$$

In *step 3*, the transitional space (x'', y'', z'') is further mapped onto the transformed space (x''', y''', z'''), as shown in Figs. 1(c)–(d). The line segment OF is compressed into OF' in z direction, and then region 3 is stretched and region 4 is compressed. It should be noted that regions 1 and 2 experience no distortions during *step* 3. The transformation equations of the four regions can be written as

Region 1:

$$x''' = x'',\ y''' = y'',\ z''' = z'' \tag{10}$$

Region2:

$$x''' = x'',\ y''' = y'',\ z''' = z'' \tag{11}$$

Region 3:

$$\begin{aligned} x''' &= x'',\ y''' = y'', \\ z''' &= -\frac{c(f-f')}{d'(f-c)}x'' - \frac{c(f-f')}{e'(f-c)}y'' + \frac{c-f'}{c-f}z'' + \frac{c(f-f')}{f-c} \end{aligned} \tag{12}$$

Region 4:

$$x''' = x'',\ y''' = y'',\ z''' = \frac{f'}{f}z'' \tag{13}$$

Combing these three steps, the transformation equations from original space to the transformed space are summarized as follows.

Region 1:

$$x''' = \frac{a-d'}{a-d}x - \frac{a(d-d')}{b(d-a)}y - \frac{a(d-d')}{c(d-a)}z + \frac{a(d-d')}{d-a},\ y''' = y,\ z''' = z \tag{14}$$

Region 2:

$$x''' = \frac{d'}{d}x,\ y''' = -\frac{b(e-e')}{d(e-b)}x + \frac{b-e'}{b-e}y - \frac{b(e-e')}{c(e-b)}z + \frac{b(e-e')}{e-b},\ z''' = z \tag{15}$$

Region 3:

$$x''' = \frac{d'}{d}x,\ y''' = \frac{e'}{e}y,\ z''' = -\frac{c(f-f')}{d(f-c)}x - \frac{c(f-f')}{e(f-c)}y + \frac{c-f'}{c-f}z + \frac{c(f-f')}{f-c} \tag{16}$$

Region 4:

$$x''' = \frac{d'}{d}x,\ y''' = \frac{e'}{e}y,\ z''' = \frac{f'}{f}z \tag{17}$$

Finally, substituting Eqs. (14)–(17) into Eq. (1), the permittivity and permeability of regions 1, 2, 3 and 4 in the first quadrant can be obtained.

Region 1:

$$\varepsilon_1 = \mu_1 = \begin{bmatrix} (A^2 + B^2C^2 + B^2D^2)/A & -BC/A & -BD/A \\ -BC/A & 1/A & 0 \\ -BD/A & 0 & 1/A \end{bmatrix} \tag{18}$$

Region 2:

$$\varepsilon_2=\mu_2=\begin{bmatrix} M/E & -FG/E & 0 \\ -FG/E & (F^2G^2+E^2+F^2H^2)/(ME) & -FH/(ME) \\ 0 & -FH/(ME) & 1/(ME) \end{bmatrix} \tag{19}$$

Region 3:

$$\varepsilon_3=\mu_3=\begin{bmatrix} M/(NI) & 0 & -JK/(NI) \\ 0 & N/(MI) & -JL/(MI) \\ -JK/(NI) & -JL/(MI) & (J^2K^2+J^2L^2+I^2)/(MNI) \end{bmatrix} \tag{20}$$

Region 4:

$$\varepsilon_4=\mu_4=\begin{bmatrix} M/(NR) & 0 & 0 \\ 0 & N/(MR) & 0 \\ 0 & 0 & R/(MN) \end{bmatrix} \tag{21}$$

where $A=(a-d')/(a-d)$, $B=(d-d')/(d-a)$, $C=a/b$, $D=a/c$, $E=(b-e')/(b-e)$, $F=(e-e')/(e-b)$, $G=b/d$, $H=b/c$, $I=(c-f')/(c-f)$, $J=(f-f')/(f-c)$, $K=c/d$, $L=c/e$, $M=d'/d$, $N=e'/e$ and $R=f'/f$.

Similarly, material parameters of the remaining parts of the concentrator can be obtained by means of axial symmetry. Taking the *xoy* plane as an example, the permeability and permeability distributions of the concentrator are shown in Fig. 2. It indicates that the permittivity and permeability tensors are spatially invariant and symmetric, and there is no singularity. These features are distinguished from the current concentrator case [23, 24], and thus greatly enhance the realizability of the concentrator in practice.

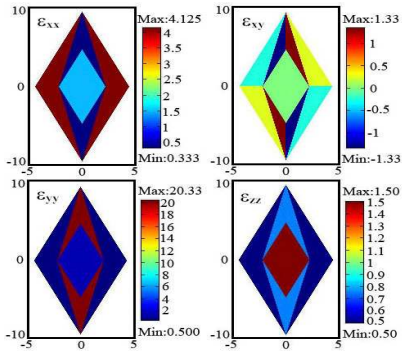

Figure 2. The permittivity and permeability distributions for the concentrator in *xoy* plane.

3. SIMULATION RESULTS AND DISCUSSION

In this section, we carry out full-wave simulations using the commercial finite element solver COMSOL Multiphysics to demonstrate the designed formulae of Eq. (18)–Eq. (21), and show the performance of the electromagnetic concentrator we develop. The geometry parameters related to the shape and size of the concentrator in the simulation are set to be $a = 4\,\mathrm{m}$, $b = 8\,\mathrm{m}$, $c = 2\,\mathrm{m}$, $d = 3\,\mathrm{m}$, $d' = 2\,\mathrm{m}$, $e = 6\,\mathrm{m}$, $e' = 4\,\mathrm{m}$, $f = 1.5\,\mathrm{m}$ and $f' = 1\,\mathrm{m}$. In the whole computational domain, both the inner and outer boundaries of the concentrator are continuous boundary conditions. The outer boundary of the domain contains four PEC boundaries and two wave ports. A 60 MHz uniform plane wave with electric field along z axis is incident onto the concentrator. S parameters and electromagnetic field distribution of the transformation devices can be flexibly obtained by using this method [13, 26].

Figure 3(a) shows the electric field (E_z) distribution in 3D profile of the concentrator when the incident wave propagates along

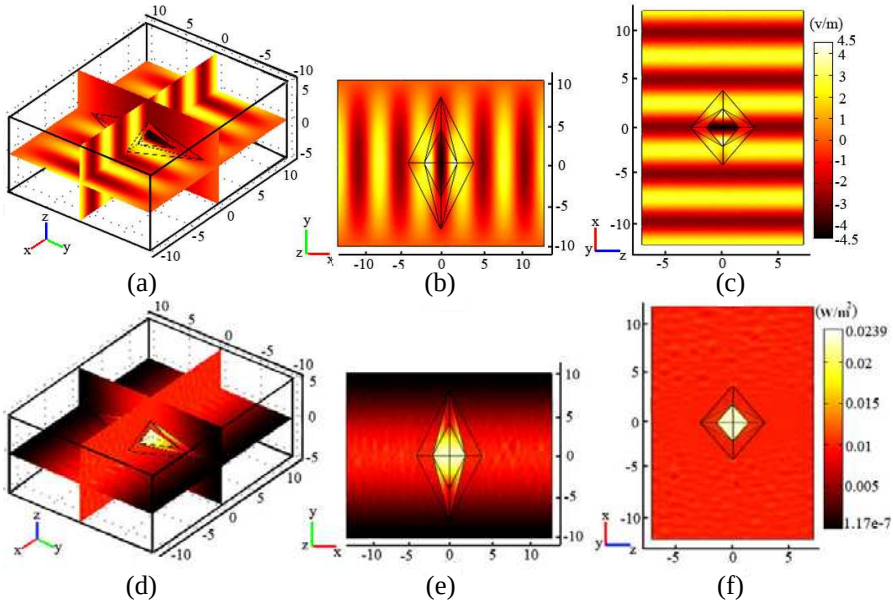

Figure 3. Electric field (E_z) distributions in the vicinity of the 3D concentrator when the incident wave propagates along x axis. (a) 3D profile; (b) xoy plane; (c) xoz plane. (d), (e) and (f) are the corresponding power flow distributions of (a), (b) and (c).

x axis. The simulation area is 25 m × 20 m × 10 m. The electric field distributions in xoy and xoz plane are illustrated in Fig. 3(b) and 3(c), respectively. It can be seen that the electromagnetic waves are focused into the compressive region when passing through the transformation region. In order to give a more convincing and clearer illustration for the electromagnetic performance of the concentrator, we further investigate the time average power flow distribution. The power flow distributions corresponding to Figs. 3(a)–(c) are shown in Figs. 3(d)–(f). From Figs. 3(d)–(f), it is obvious that the power flow in the compressive region is spatially uniform and strongly enhanced. It confirms the effectiveness of the material parameters we develop.

To study the influence of wave direction on the performance of the concentrator, electric field (E_z) and power flow distributions are simulated when the incident wave propagates along the y axis. Results are shown in Fig. 4, where the simulation area is 20 m × 25 m × 10 m. From Figs. 4(a)–(c), we can observe that the incident waves are perfectly focused by the concentrator into the compressive region without any distortion. The corresponding power flow distributions

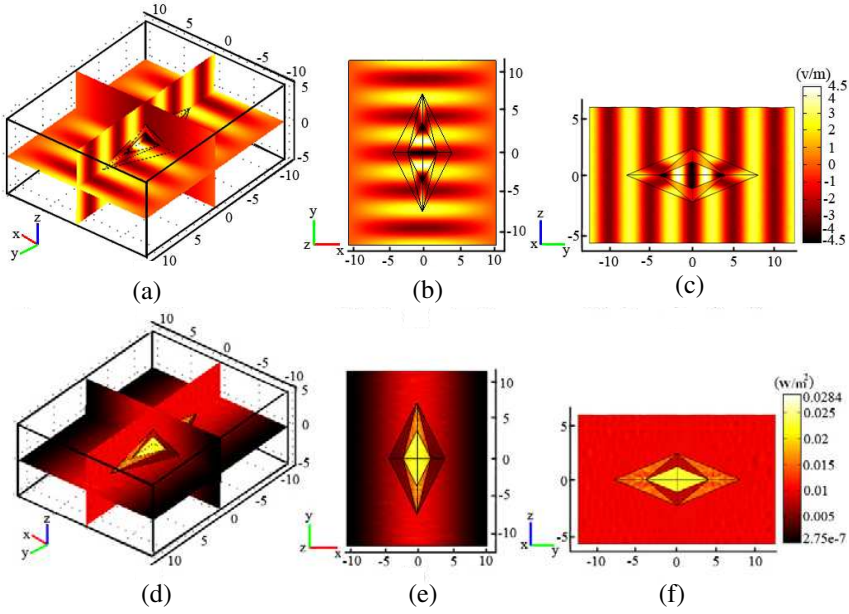

Figure 4. Electric field (E_z) distributions in the vicinity of the 3D concentrator when the incident wave propagates along y axis. (a) 3D profile; (b) xoy plane; (c) yoz plane. (d), (e) and (f) are the corresponding power flow distributions of (a), (b) and (c).

shown in Figs. 4(d)–(f) are strongly enhanced. Therefore, the performance of the concentrator is independent on the direction of the wave. Interestingly, much stronger power flow enhancements can be achieved by diminishing the size of the compressive region through decreasing the ratio of $d'/d = e'/e = f'/f = \tau$. The power flow distribution along z axis for different values of τ is plotted in Fig. 5. It is seen that the power flow of the compressive region with $\tau = 1/6$ is about 16 times that of the compressive region with $\tau = 2/3$. The enhancement theoretically diverges to infinity as the volume of the compressive region goes to zero.

Since almost 95% of the solar radiation is concentrated within the wavelength range from 250 nm to 2500 nm, solar concentrators should operate in a wide spectral range. Fig. 6 shows the power flow distributions of the concentrator for the different frequency. It can be seen that the power flow distribution in the compressive region keeps unchanged within ten octave bandwidth. Therefore, based on coordinate transformation method, the concentrator can operate in a wide bandwidth. Similar broadband properties of cloak have been confirmed by Wang et al. [26] using linear transformation. The "step-like" pattern is believed to be induced by the numerical method due to discretization. It can be improved by fine mesh with the cost of memory consumption and computation time. With the development of metamaterial technology, if the concentrator is designed to work in optical frequency range, high efficiency conversion of solar energy could be achieved.

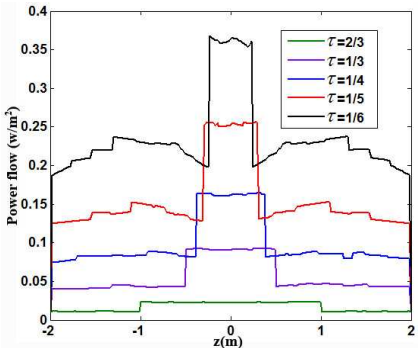

Figure 5. Power flow distribution along z axis for the different values of τ.

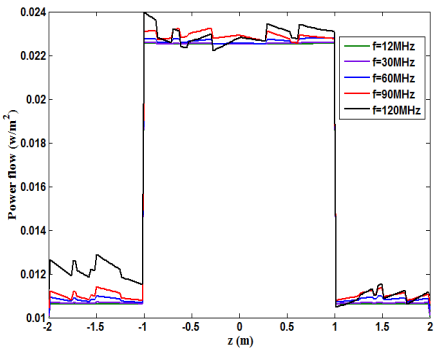

Figure 6. Power flow distribution along z axis for different frequency.

4. CONCLUSION

Based on a three-step coordinate transformation method, a 3D diamond-shaped concentrator is proposed in this paper. The relative permittivity and permeability tensors are derived, and verified by full-wave simulation. The linear coordinate transformation avoids the singularity in the material parameters. Moreover, due to homogeneously stretching and compressing at the orthogonal directions during the transformation, the resulted material parameters are homogeneous. Simulation results show that the performance of the concentrator is in dependent on the directions of the incident wave, and it operates in a wide spectral range. It is expected that our works are helpful for speeding up the applications of the concentrators in solar cells or similar devices where high field intensity are required.

ACKNOWLEDGMENT

This work was supported by the National Natural Science Foundation of China (Grant No. 60861002), Training Program of Yunnan Province for Middle-aged and Young Leaders of Disciplines in Science and Technology (Grant No. 2008PY031), the Scientific Research Foundation of Yunnan University (Grant No. 2010YB025), and the Technology Innovation and Entrepreneurship Plan for Students of Yunnan University.

REFERENCES

1. Pendry, J. B., D. Schurig, and D. R. Smith, "Controlling electromagnetic fields," *Science*, Vol. 312, No. 5781, 1780–1782, 2006.
2. Schurig, D., J. J. Mock, B. J. Justice, S. A. Cummer, J. B. Pendry, A. F. Starr, and D. R. Smith, "Metamaterial electromagnetic cloak at microwave frequencies," *Science*, Vol. 314, No. 5801, 977–980, 2006.
3. Weder, R., "A rigorous analysis of high-order electromagnetic invisibility cloaks," *J. Phys. A: Math. Theor.*, Vol. 41, No. 6, 065207, 2008.
4. Weder, R., "The boundary conditions for point transformed electromagnetic invisibility cloaks," *J. Phys. A: Math. Theor.*, Vol. 41, No. 41, 415401, 2008.
5. Leonhardt, U. and T. Tyc, "Broadband invisibility by non-euclidean cloaking," *Science*, Vol. 323, No. 5910, 110–112, 2009.

6. Liu, R., C. Ji, J. J. Mock, J. Y. Chin, T. J. Cui, and D. R. Smith, "Broadband ground-plane cloak," *Science*, Vol. 323, No. 5912, 366–369, 2009.
7. Ma, H. F. and T. J. Cui, "Three-dimensional broadband ground-plane cloak made of metamaterials," *Nature Communication*, Vol. 1, 21, 2010.
8. Chen, H. Y., C. T. Chan, and P. Sheng, "Transformation optics and metamaterials," *Nature Materials*, Vol. 9, 387–396, 2010.
9. Lai, Y., H. Y. Chen, Z. Q. Zhang, and C. T. Chan, "Complementary media invisibility cloak that cloaks objects at a distance outside the cloaking shell," *Phys. Rev. Lett.*, Vol. 102, No. 9, 093901, 2009.
10. Cheng, Q., W. X. Jiang, and T. J. Cui, "Investigations of the electromagnetic properties of three-dimensional arbitrarily-shaped cloaks," *Progress In Electromagnetics Research*, Vol. 94, 105–117, 2009.
11. Yang, C. F., M. Huang, J. Yang, Z. Xiao, and J. Peng, "An external cloak with arbitrary cross section based on complementary medium," *Progress In Electromagnetics Research M*, Vol. 10, 13–24, 2009.
12. Ma, H., S. B. Qu, Z. Xu, and J. F. Wang, "The open cloak," *Appl. Phys. Lett.*, Vol. 94, 103501, 2009.
13. Yang, J. J., M. Huang, C. F. Yang, and J. Yu, "Reciprocal invisibility cloak based on complementary media," *Eur. Phys. J. D*, Vol. 61, No. 3, 731–736, 2011.
14. Wang, W., L. Lin, X. F. Yang, J. H. Cui, C. L. Du, and X. G. Luo, "Design of oblate cylindrical perfect lens using coordinate transformation," *Opt. Express*, Vol. 16, No. 11, 8094–8105, 2008.
15. Chen, H. Y. and C. T. Chan, "Transformation media that rotate electromagnetic fields," *Appl. Phys. Lett.*, Vol. 90, No. 24, 241105, 2007.
16. Rahm, M., D. Schurig, D. A. Roberts, S. A. Cummer, D. R. Smith, and J. B. Pendry, "Design of electromagnetic cloaks and concentrators using form-invariant coordinate transformations of Maxwell's equations," *Photon. Nanostruct. Fundam. Appl.*, Vol. 6, No. 1, 87–95, 2008.
17. Lai, Y., J. Ng, H. Y. Chen, D. Z. Han, J. J. Xiao, Z. Q. Zhang, and C. T. Chan, "Illusion optics: The optical transformation of an object into another object," *Phys. Rev. Lett.*, Vol. 102, 253902, 2009.

18. Yang, C. F., J. J. Yang, M. Huang, J. H. Peng, and G. H. Cai, "Two-dimensional electromagnetic superscatterer with arbitrary geometries," *Comput. Mater. Sci.*, Vol. 49, No. 4, 820–825, 2010.
19. Rahm, M., S. A. Cummer, D. Schurig, J. B. Pendry, and D. R. Smith, "Optical design of reflectionless complex media by finite embedded coordinate transformations," *Phys. Rev. Lett.*, Vol. 100, No. 6, 063903, 2008.
20. Jiang, W. X., J. Y. Chin, and T. J. Cui, "Anisotropic metamaterial devices," *Materialstoday*, Vol. 12, No. 12, 26–33, 2009.
21. Kwon, D. H. and D. H. Werner, "Transformation electromagnetics: An overview of the theory and applications," *IEEE Antennas and Propagation Magazine*, Vol. 52, No. 1, 24–46, 2010.
22. Jiang, W. X., T. J. Cui, Q. Cheng, J. Y. Chin, X. M. Yang, R. Liu, and D. R. Smith, "Design of arbitrarily shaped concentrators based on conformally optical transformation of nonuniform rational B-spline surfaces," *Appl. Phys. Lett.*, Vol. 92, 264101, 2008.
23. Yang, J. J., M. Huang, C. F. Yang, Z. Xiao, and J. H. Peng, "Metamaterial electromagnetic concentrators with arbitrary geometries," *Opt. Express*, Vol. 17, No. 22, 19656–19661, 2009.
24. Yang, C. F., J. J. Yang, M. Huang, J. H. Peng, and W. W. Niu, "Electromagnetic concentrators with arbitrary geometries based on Laplace's equation," *JOSA A*, Vol. 27, No. 9, 1994–1998, 2010.
25. Li, W., J. G. Guan, and W. Wang, "Homogeneous-materials-constructed electromagnetic field concentrators with adjustable concentrating ratio," *J. Phys. D: Appl. Phys.*, Vol. 44, 125401, 2011.
26. Wang, X. H., S. B. Qu, X. Wu, J. F. Wang, Z. Xu, and H. Ma, "Broadband three-dimensional diamond-shaped invisible cloaks composed of tetrahedral homogeneous blocks," *J. Phys. D: Appl. Phys.*, Vol. 43, 305501, 2010.
27. Schurig, D., J. B. Pendry, and D. R. Smith, "Calculation of material properties and ray tracing in transformation media," *Opt. Express*, Vol. 14, No. 21, 9794–9804, 2006.